

Optimum Synthesis and Characterization of Precursor Solution for a Hard Coating Silica Film Prepared by Sol-Gel Process

Sun-Il Kim,^{*} Gu-Yeol Kim, Hyung-Mi Lim, Bong-Woo Lee,[†] and Jae-Woon Nah[‡]

Department of Chemical Engineering, Chosun University, Kwangju 501-759, Korea

[†]Technical Institute of Kun-Sul Chemical, Kyungki-do 435-030, Korea

[‡]Department of Polymer Science and Engineering, Sunchon National University, Chonnam 540-742, Korea

Received April 4, 2000

Crack-free hard coating silica films were prepared by sol-gel process from two kinds of silicon alkoxide (tetraethoxysilane and methyltrimethoxysilane) and two kinds of alcohol (methanol and isopropyl alcohol) with an acid catalyst, acetic acid. A silicate framework of the precursor solution was investigated by infrared spectroscopy (IR) in the process of hydrolysis and condensation. The extent of the condensation in the intermediates was elucidated by gel permeation chromatography (GPC) and ²⁹Si-NMR spectroscopy. The hard coating films were characterized by IR, scanning electron microscope (SEM), thermo gravimetric analyzer (TGA) and differential scanning calorimeter (DSC). The synthetic condition for the crack-free and transparent silica film formation was optimized in terms of starting materials for the precursor solution as well as preparation method of the silica film.

Introduction

Plastics and polymer have been widely used as materials for optics, electronics, construction, and car parts due to its characteristics of light weight, easy processability, and non-corroding behavior.¹ Those materials often need post-processing such as applying hard coating on the surface, to increase the chemical and mechanical durability or to introduce specific functionality. There are three different types of functional coating materials. One is organic coating material as melamine, acryl, and urethane. Another is inorganic material as silicon compounds. The other is organic-inorganic hybrid composite,^{2,3} which have shown many interesting mechanical, optical, and thermal properties. One of the simplest system in the hybrid materials, methyl-modified silicate materials were used to obtain a crack-free, well-defined, and characterized microporous thin films.⁴ Many different methods for the synthesis of powder, or bulk porous materials or microporous thin films have been developed, however, these can not be used to prepare continuous, pinhole-free, transparent, and crack-free hard coating thin film. Sol-gel process in the preparation of the coating films is known to be relatively easy to prepare. In addition, it provides uniform surface throughout the substrate, and improves the surface property by changing mechanical or chemical properties and thereby providing optic, electromagnetic, or catalytic qualities. Also it was found easy to produce ceramic thin films ranging in characteristics dense to highly porous layers.⁵ The control of porosity has a special interest on the preparation of chemically enforced materials^{6,7} or selective chemical sensors^{4,8} or membrane.^{9,10} On the other hand, high density and hardness are the required properties for the purpose of protection as a hard coating material. Here we focused on finding the synthesis condition of precursor solution to produce the transparent crack-free hard coating film starting from the two kinds of silicon alkoxide, tetra-

ethoxysilane and methylmethoxysilane.

It has been widely studied about the various synthetic parameters in the sol-gel synthesis, usually focused on how to be correlated with rate and degree of hydrolysis and condensation as well as density and porosity of the final film.^{5,11} These synthetic parameters of precursor solution are the kind of silicon alkoxide, the concentration and molar ratio of starting reagents, catalyst, pH (which depends on the kind and amount of catalyst), temperatures and time (reaction, ageing, and drying), and viscosity at the moment of deposition, which were examined to see how to effect on the formation of crack-free transparent hard coating film in this study. Other possible factors in the step of coating procedure, such as the coating method, drying, and heating conditions, were studied to characterize the morphology of the film surface and to correlate with the crack formation. Finally, we investigated the silica framework of the final hard coating film and its thermal stability.

Experimental Section

Precursor solution of coating films was prepared as follows. Tetraethoxysilane (TEOS, Wako, 95%) and methyltrimethoxysilane, (MTMS, Shinetsu, 98.9%) were combined with methanol (MeOH, Aldrich, 99%) and isopropylalcohol (IPA, Fisher Scientific) and stirred using magnetic stirrer. The mixture of distilled water and a catalyst was carefully and slowly added, using a dropping funnel, for 60 min to the above mixture of silicon alkoxides and alcohols under vigorous stirring in ice bath. The molar ratio of TEOS + MTMS : IPA + MeOH : catalyst : distilled water was 1 : 0.278 : 0.077 : x, where x = 2.92, 3.95, and 4.74. The molar ratio of TEOS : MTMS was 1 : 8, 1 : 1, and 8 : 1 and IPA : MeOH was 1 : 0.82. Three different catalysts, acetic acid (Junsei, 99%), HCl, and NH₄OH were used. All reagents were used without a further purifica-

tion. The mixture solution after addition of the catalyst was removed from ice bath and stirred at room temperature for 60 min after the temperature was equilibrated to room temperature, which took about 30 min. The solution was heated slowly to 60 °C for 30 min (speed of 2 °C/min) and reflux at 60 °C for 60 min, and cooled to room temperature, which took another 30 min. For the convenience of nomination of samples, it was distinguished with overall reaction time. The initial point of reaction was considered as the moment when the acid catalyst was added to the mixture of alkoxides and alcohols. Therefore, the overall reaction time 0-60 min is during addition of the catalyst, 60-90 min during the temperature equilibrated to room temperature, 90-150 min at room temperature, 150-180 min during heating to 60 °C and 180-240 min heating at 60 °C. Each step was carried out under nitrogen gas flux. The precursor solution was stored at 5 °C to examine the ageing effect before deposition on a substrate. A catalyst, dibutyltin dilaurate (DBTDL, Aldrich, 95%) was added to the precursor solution by 0.2% and stirred for 30 min at room temperature vigorously, just before deposition to the glass plates.

Glass plate was used as a substrate for the coating. The glass plate was ultrasonically cleaned with THF, benzene, and water for 5 min respectively. Coating films on the glass plate were prepared by flow coating or dip coating method, after filtering with a syringe filter (DAE HA MEDICAL Corp., 0.45 μ m). The flow coating was performed once or many times and dried in vertical direction, but the dip coating was done only once for each film and dried on horizontal direction after it was withdrawn in a vertical direction. The coating films on glass plate were typically dried at room temperature for 20 min and heated at 180 °C for 30 min. After heating the films at 180 °C, they were cooled to room temperature slowly.

Infrared (IR) absorption spectra of the precursor solution at various reaction time and the coating films were measured using an FT-IR spectrophotometer (IFS66, Bruker). A drop-let of the precursor solution was sampled on NaCl cell and spreaded evenly. On the other hand, a small portion of the film was scrapped off, grounded, mixed with KBr, and pelletized for IR analysis for the coating film samples. The distribution of molecular weight for reaction intermediates was studied by gel permeation chromatography (GPC). Flux rate and concentration of the sample was 1.0 mL/min and 8.34 mg/mL of tetrahydrofuran. The OH group in the intermediate mixture solutions at overall reaction time 120 min and 210 min was capped by addition of the mixture of trimethylchlorosilane (TMCS, Acros organics) and pyridine in 1 : 1 ratio. Then, precipitates were separated by centrifuge.²⁹Si NMR spectrum was taken with 300 MHz FT-NMR (Varian, UNITY plus 300) at 59.611 MHz for the precursor solution at overall reaction time 120 min after capping procedure. The surface morphology of coating films were examined by a scanning electron microscope (SEM, JSM840A). The thickness of the coating films was evaluated by observing the cross section of the films on glass substrate using SEM. Thermal analysis was performed by thermo gravimetric analyzer (TGA) and

differential scanning calorimeter (DSC) to investigate the thermal stability of coating films at a heating rate of 10 °C/min under oxygen gas flux from 100 °C to 800 °C.

Results and Discussion

Optimization of the synthetic condition and the coating procedure. The transparent and crack free coating film was obtained only when acetic acid was used as catalyst in this study. Several typical conditions given in Table 1 represent molar ratio of starting material and type of catalyst. When the HCl was used as catalyst in the same concentration as acetic acid, the precursor solution of C_{HCl} lost its transparency after complete addition of HCl. In the case of NH_4OH catalyst, it lost transparency soon after initial addition of the catalyst. The hydrolysis in sample $C_{a.a.}$ was slowed down with acetic acid, and also it was further equipped with ice bath to control the speed of hydrolysis. The water content in the synthesis of precursor solution was found optimized when the molar ratio of water was 3.95, among three different ratios tried in this experiment. The crack appeared in the case of lower water content and the clearness was lower in the case of higher water content, due to the fast hydrolysis.⁶ The ratio of TEOS and MTMS was known to effect on the hardness of the film. The 1 : 1 ratio gave more brittle film than 1 : 8 ratio, even though it was still transparent. The wetting property on the glass substrate of samples was not as good as that of $C_{a.a.}$ sample. The viscosity was found to be important factor on the formation of crack. In general, too low or too high viscosity caused crack easily. Not only these factors from the precursor solution, but also the coating procedure or after-treatment affected on the formation of crack. The thickness of the film was one of well known factors in the formation of crack. The thicker the film, the more brittle the film.^{5,11} It was suggested that the effect of substrate during the drying of the supported thin layers oppose the shrinkage of the coating.⁵ A thick film prepared with high viscosity precursor solution was found brittle in the current experiment, and it may lead to the same conclusion that the thick film is less effective of preventing a crack. The coating method itself gives some difference in the crack formation. From the precursor solution in the same viscosity, the flow coating method could result to the less brittle film than the dip coating method. When the film was prepared without

Table 1. Molar ratio of precursor solution samples prepared in this experiment. Catalyst was acetic acid (a.a.), HCl, and NH_4OH

Sample name	TEOS + MTMS	IPA + MeOH	Catalyst	Water
$C_{a.a.}$	1 (1:8)	0.278 (1:0.82)	0.077 (a.a.)	3.95
C_{HCl}	1 (1:8)	0.278 (1:0.82)	0.077 (HCl)	3.95
C_{NH_4OH}	1 (1:8)	0.278 (1:0.82)	0.077 (NH_4OH)	3.95
W_{low}	1 (1:8)	0.278 (1:0.82)	0.077 (a.a.)	2.92
W_{high}	1 (1:8)	0.278 (1:0.82)	0.077 (a.a.)	4.74
S_1	1 (1:1)	0.278 (1:0.82)	0.077 (a.a.)	3.95
S_2	1 (8:1)	0.278 (1:0.82)	0.077 (a.a.)	3.95

ageing, the crack was sometimes formed in the film prepared by the dip coating method. However, the flow coating method was found to prevent cracks more effectively since it probably gives a thinner film than the dip coating method in this experiment.

Infrared and ^{29}Si -NMR investigations of the silicate precursor solution. The precursor solution for the $\text{C}_{a,a}$ sample was studied by infrared spectra in the process of hydrolysis and condensation. The spectra at various reaction time have been plotted in Figure 1. The first spectrum, Figure 1(a) was taken for the mixture solution of TEOS, MTMS, MeOH, and IPA, just before the addition of acid and water mixture. The successive spectra were taken after the addition of acid, where characteristic peaks for hydrolysis and condensation changed with time. The broad absorption band at about $3000\text{--}3700\text{ cm}^{-1}$ corresponds to the fundamental stretching vibrations of isolated and H-bonded SiO-H and hydrogen-bonded molecular water.¹¹ The sharp peak at 2975 cm^{-1} is assigned to stretching vibrations for aliphatic C-H bonds. $1600\text{--}1700\text{ cm}^{-1}$ peaks are assigned to C-H and H_2O . Absorption bands at 1270 and $1040\text{--}1090\text{ cm}^{-1}$ are assigned to Si-O-Si asymmetric modes. The absorption band at 790 cm^{-1} is associated with symmetric Si-O-Si stretching or vibrational modes of ring structures.¹¹ The peak appeared about 20 min after acid addition at 905 cm^{-1} and it may be assigned to Si-OH stretching vibration. It was reported to be found at 960 cm^{-1} in the system of hydrolysis of TEOS¹¹ and shifted to 930 cm^{-1} in the hybrid film prepared from a coating solution derived from TEOS and MTMS mixture in 1 : 3 ratio.⁴ Since it was found further shifted to 905 cm^{-1} in the current hybrid film prepared from TEOS and MTMS in 1 : 8 ratio, the

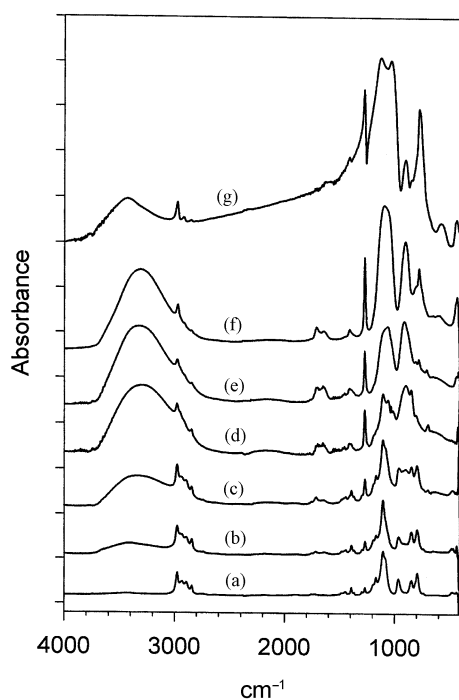


Figure 1. IR spectra at various overall reaction time. (a) 0 min, (b) 10 min, (c) 20 min, (d) 40 min, (e) 150 min, (f) 240 min, (g) final film prepared as in Table 1.

Table 2. The relative absorbance of several characteristic peaks compared to CH absorbance (at 2975 cm^{-1}) in the process of synthesis

Sample		Relative absorbance at given wavenumber, cm^{-1}					
Reaction condition	Overall reaction time (min)	3000 ~3700	1710	1270	1040 ~1090	905	790
Ice bath	10	0.44	0.22	0.56	1.89	0.00	1
	20	0.73	0.17	0.53	1.47	0.00	0.77
	40	1.29	0.29	0.9	1.19	1.33	0.81
Room temp.	90	1.83	0.42	1.33	1.67	2.08	1.25
	150	1.73	0.40	1.46	1.76	1.87	1.03
60 °C	180	2.15	0.30	1.70	2.52	2.30	1.41
	240	2.04	0.39	2.32	3.57	2.75	2.00
5 °C	1 week	1.75	0.33	2.83	4.67	2.92	2.67
Coating film		1.09	1.36	3.91	4.73	2.09	3.36

larger amount of MTMS in the hybrid silicate, the lower wavenumber of Si-OH stretching vibration. After all, infrared spectrum of the coating film, prepared as condition given in Table 3(e) is shown in Figure 1(f), where the greatest Si-O-Si peaks tell that the condensation process was further progressed after the deposition on the glass.

The relative absorbance of several characteristic peaks compared to CH absorbance (at 2975 cm^{-1}) in the process of synthesis are summarized in Table 2 and Figure 2. The sample stored at 5 °C for a week was labelled as the sample at overall reaction time 340 min and the final film sample as overall reaction time 370 min in Figure 2. It shows that the relative absorbance changes in the process of reaction, which might give some insight of reaction mechanism. The absorbance for SiO-H peak at $3000\text{--}3700\text{ cm}^{-1}$ increased with the addition of acid in water, which indicate the procession of hydrolysis. After completion of dropping acids in the mixture of TEOS + MTMS + MeOH + IPA, there is slight decrease in the SiO-H peak throughout the period to the formation of coating film, which indicate that the amount of SiO-H decreased with time while the condensation progressed after completion of addition of acid. There is also some decrease in the Si-OH peak in the final film. There is only slight increase in absorbance at 1700 cm^{-1} throughout the reaction. However, the characteristic peaks for Si-O-Si at 1270 , $1040\text{--}1090$, and 790 cm^{-1} increased throughout the process, especially increased greater during the process of acid addition and heating. The Si-O-Si asymmetric peak in the range of $1040\text{--}1090\text{ cm}^{-1}$ appears after 40 min in ice bath and shifts toward lower wavenumber with time. During the period of ageing the precursor solution at 5 °C for a week, condensation proceeded very slowly as shown in Table 2.

The OH group in the precursor solution at the overall reaction time 120 min was capped by trimethoxysilane group and capping was checked by IR spectra in Figure 3. The characteristic peaks of SiO-H and Si-OH stretching vibrations at $3000\text{--}3700\text{ cm}^{-1}$ and 905 cm^{-1} disappeared after the capping procedure, which confirm the OH group in the precursor solution was effectively reduced and the condensation

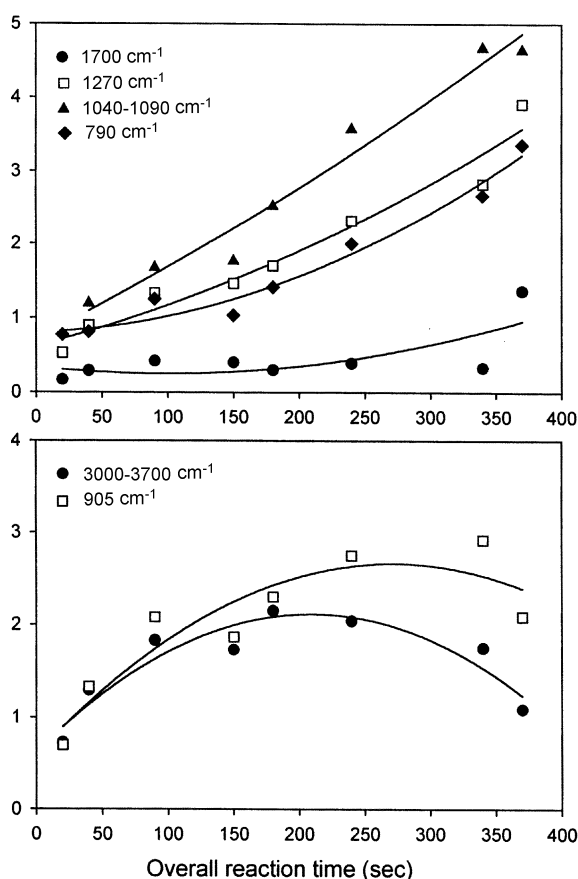


Figure 2. The relative absorbance of several characteristic peaks compared to CH absorbance (at 2975 cm^{-1}). The overall reaction time is measured from the moment of addition of acid catalyst. The sample at overall reaction time 340 min is for the precursor solution stored at 5°C for a week and one at 370 min is for the film sample. The curve is just to guide an eye for the trend.

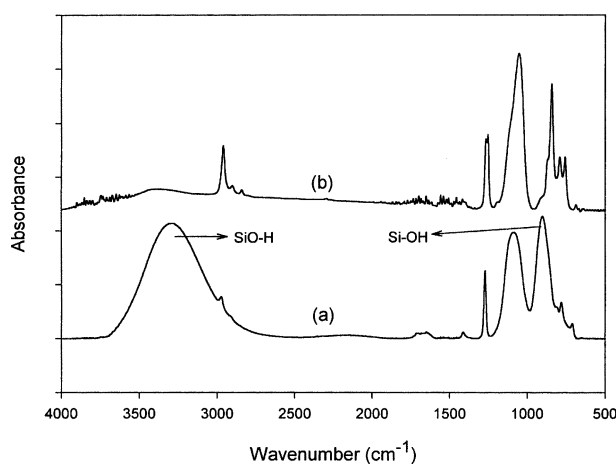


Figure 3. IR spectra of intermediates (a) before and (b) after the capping procedure.

must have not progressed further. Weight mean molecular weight for the capping solutions was found to be 383 and 391 for samples at the overall reaction time 120 min and 210 min.

The degree of condensation could be analyzed by ^{29}Si -

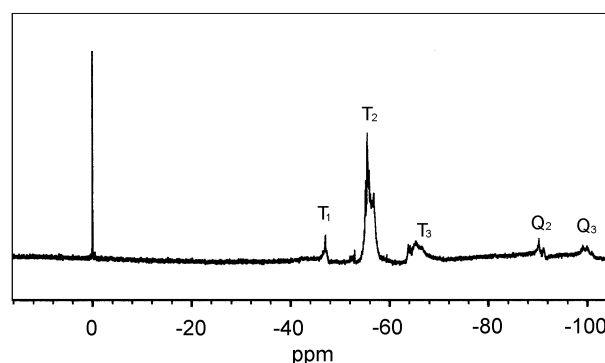


Figure 4. ^{29}Si -NMR spectrum of the precursor solution synthesized from TEOS + MTMS (1 : 8) + IPA + MeOH (1 : 0.82).

NMR spectroscopy in Figure 4, which revealed five different types of ^{29}Si peaks, T_1 , T_2 , T_3 , Q_2 , and Q_3 , where T_n denotes for $\text{CH}_3\text{-Si}(\text{OSi})_n\text{O}_{3-n}$ and Q_n denotes for $\text{Si}(\text{OSi})_n\text{O}_{4-n}$ from MTMS and TEOS origin, respectively. It was taken at room temperature for the precursor solution at overall reaction time 120 min after capping. The relative area of $T_1 + T_2 + T_3 : Q_2 + Q_3$ is about 8 : 1 as the ratio of MTMS and TEOS as starting material. It is worth to note that the distributions of T_n and Q_n are different, where average of n is higher in the case of Q_n . It can be concluded that the condensation degree of TEOS was greater than that of MTMS from the distribution of T_n and Q_n peaks.

Surface morphology and thermal stability of the silica film. We failed many trials to obtain the film without a crack. In most cases, the film revealed a crack in the process of heating if the film was prepared by dip coating method. Figure 5 shows various morphology of the coating film surfaces prepared from the precursor solution 'C_{aa}' without any crack in different ageing, drying, heating conditions and by different coating methods as summarized in Table 3. The surface of the coating film depends on the coating method and after-treatment as well as the synthesis condition of the precursor solution. The heat treatment (30 min at 180°C) resulted the difference in a pore size and shape as can be compared in Figure 5(a) and 5(b). The pores were formed spherical and larger than those in the film after heating at 180°C for 30 min. The pores started to evolve in the precursor solution in the drying process after it was applied on the substrates. It seems that the heating stopped the process of pore evolution and the pores, which was under the process of forming, was fixed at a certain moment of heating and ended up with nonspherical shape. The effect of ageing of solution at 5°C before deposition on the substrate can be shown in Figure 5(d) and 5(f). After ageing the precursor solution for a week at 5°C , the surface of the coating film did not show any pores. However, after ageing two weeks, the protuberances were observed. Therefore, we could assume the densification of the microstructure during the ageing process. The difference of coating method caused expected difference in the size and shape of pores as shown in Figure 5(c) and 5(d). The dip coating method produced the larger pore on the surface of the film. The thickness of the film was measured to

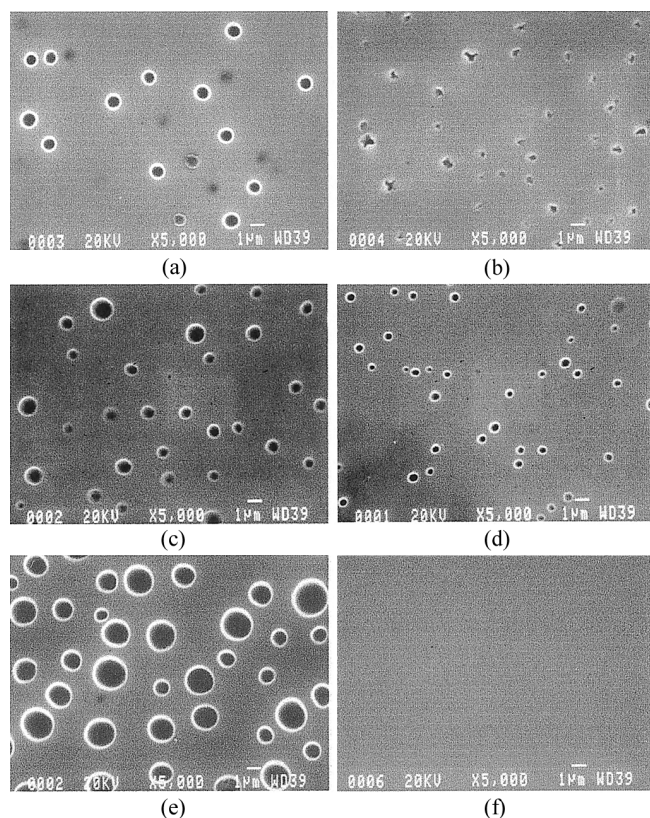


Figure 5. SEM images of the coating films prepared in various ageing, drying, heating conditions, as summarized in Table 1.

be 11 μm and 4 μm for the film (c) and (d) by observing a cross section of the film on a substrate using SEM. Even with the same dip coating method, the pores are larger in the case that the film was withdrawn more slowly as shown in Figure 5(e), where the thickness of the film was 25 μm . It is assumed that the pores are getting larger with the thickness of the film. Since the flow coating method was found to be more effective to prevent a crack, it is opposed to a general trend that the larger the pore, it is easier to prevent a crack formation. It is interesting to note that the surface of the film, prepared as the film in Table 3(c) but dried at room temperature in vertical position, is the same as Figure 5(f). This suggests that the gravitational force prevent the pore evolution in addition to that, dip coating method allow the surface property different from flow coating method. The thickness of the film prepared by dip coating and dried in vertical position was 4 μm as was prepared by flow coating method. Therefore, the difference of pore sizes in Figure 5(c), 5(d), 5(e) was not solely from the difference of thickness of the films. The higher porosity of the film was observed in the thin film rather than in thick self supported film in the case of Klotz *et al.*'s experiment⁵ but the opposite trend was observed in our experiment as shown in Figure 5(c), (d), (e). In spite of the substrate effect of preventing shrinkage of the precursor solution, the pores are the smallest in the thinnest film. It indicate that there were not only substrate effect but also the force evolving a pore in the thicker film while condensation progress.

Table 3. Preparation time and coating method of films on a glass substrate prepared from the precursor solution 'C_{aa}'

Sample	Ageing at 5 °C	Drying at RT	Heating at 180 °C	Coating method
a	0	over 1 day	0	flow coating (repeated)
b	0	20 min	30 min	flow coating (repeated)
c	0	20 min	30 min	dip coating (fast withdraw)
d	0	20 min	30 min	flow coating (once)
e	0	20 min	30 min	dip coating (slow withdraw)
f	1 week	20 min	30 min	flow coating (once)

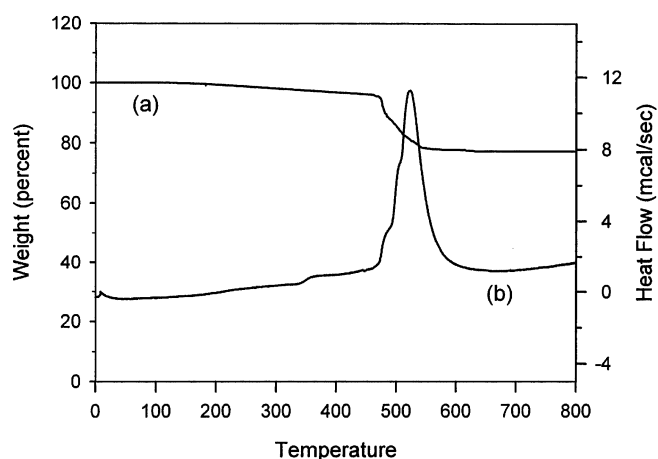


Figure 6. (a) TGA and (b) DSC curves of the coating film at a heating rate of 10 °C/min.

TGA and DSC curves of the coating film, prepared as in Table 3(f), are shown in Figure 6. It indicated a large exotherm and weight loss between 460–600 °C. In many other silica films, large weight loss was found around 250 °C, which was ascribed to the organic surfactants during calcination.^{12,13} In our experiment, the weight loss was 0.03% at 183 °C, 4.7% at 471 °C, and finally large overall weight loss between 460–600 was about 22.8%. The coating film revealed thermal stability up to 460 °C. We attribute the small weight loss at 183 °C to the decomposition of residual solvents and the large exotherm above 460 °C to the decomposition of alkyl groups of organosilane, respectively.

Conclusion

The synthesis condition was optimized for a transparent crack-free hard coating film, which was prepared by sol-gel process from the mixed silicon alkoxides. The molar ratio of TEOS + MTMS : IPA + MeOH : acetic acid : distilled water was 1 : 0.278 : 0.077 : 3.95, where TEOS : MTMS was 1 : 8 and IPA : MeOH was 1 : 0.82. The thickness of the film obtained without a crack was 4–25 μm . The degree of condensation of TEOS was greater than that of MTMS from the distribution of T_n and Q_n peaks in ²⁹Si-NMR spectrum. The control of initial hydrolysis step during acid addition was important factor to obtain crack-free and transparent hard coating film. The crack on the hard coating film was effec-

tively prevented when the precursor solution was applied on a substrate at an appropriate viscosity. Not only the viscosity but also the coating method and after-treatment was found to give effect on the formation of crack. Thermal stability of the film was found to be quite good up to the temperature 460 °C.

Acknowledgment. We are greatly indebted to the Korea Research Foundation for the financial support made for this work in the program year of 1998 and also supported in part by research funds of Chosun University (1995).

References

1. Paul, S., In *Surface Coatings*; Paul, S., Ed.; John Wiley & Sons Ltd: West Sussex, England, 1996; p 487.
 2. Schbert, U.; Husing, N.; Lorenz, A. *Chem. Mater.* **1995**, 7, 2010.
 3. Krug, H.; Merl, N.; Schmidt, H. *J. Non-Cryst. Solids* **1992**, 147, 447.
 4. Yan, Y.; Hoshino, Y.; Duan, Z.; Chaudhuri, R.; Sarkar, A. *Chem. Mater.* **1997**, 9, 2583.
 5. Klotz, M.; Ayrat, A.; Guizard, C.; Cot, L. *Bull. Korean Chem. Soc.* **1999**, 20, 879.
 6. Monde, T.; Fukube, H.; Nemoto, F.; Yoko, T.; Konakahara, T. *J. Non-Cryst. Solids* **1999**, 246, 54.
 7. Tadanaga, K.; Azuta, K.; Minami, T. *J. Ceramic Soc. Jap.* **1997**, 105, 555.
 8. Hoekstra, K. J.; Bein, T., *Chem. Mater.* **1996**, 8, 1865.
 9. (a) Nair, B. N.; Elferink, W. J.; Keizer, K.; Verweij, H. *J. Colloid Interface Sci.* **1996**, 178, 565. (b) Nair, B. N. I.; Yamaguchi, T.; Okubo, T.; Suematsu, H.; Keizer, K.; Nakao, S.-I. *J. Mem. Sci.* **1997**, 135, 237.
 10. Piaggio, P.; Bottino, A.; Capannelli, G.; Carosini, E. *Langmuir* **1995**, 11, 3970.
 11. Brinker, C. J.; Scherer, G. W. *Sol-Gel Science, the Physics and Chemistry of Sol-Gel Processing*; Academic Press: Boston, 1990.
 12. Yang, H.; Coombs, N.; Ozin, G. A. *J. Mater. Chem.* **1998**, 8, 1205.
 13. Rho, H.-S.; Chang, J.-S.; Park, S.-E. *Korean J. Chem. Soc.* **1999**, 16, 331.
-